V Glycerol Modified PEDOT:PSS in P3HT:PCBM solar cells

Despite the significant development of small scale polymer based photovoltaics, one limiting factor that remains to be resolved is the loss of photovoltaic efficiency on scale-up to large area. This loss is due to the relatively high sheet resistance of the anode, typically indium tin oxide. The conductive polymer PEDOT:PSS is often used in conjunction with ITO and it has been shown that the addition of secondary additives to PEDOT:PPS can greatly reduce its sheet resistance. In this chapter the use of glycerol modified PEDOTP:PSS as a highly conductive anode in P3HT:PCBM solar cells is investigated. The results show no improvement in device efficiency due to the addition of glycerol. However, it does introduce some interesting device physics which highlight the need for accurate experimental design when testing novel device efficiencies.

V.I Background

Considerable effort has been directed towards the discovery of a replacement for ITO in all manner of polymer based electronics due to its high and increasing cost, and sub-optimal resistivity. The bulk of these efforts have focused on the identification of an alternative transparent conducting oxide (TCO) containing less expensive constituents.[1,2,3] In addition, a polymer-based replacement has also been

sought, in line with the desire for 'all-organic' electronic devices. A number of avenues have been investigated including carbon nanorods, graphene and modified conductive polymers such as PEDOT:PSS.[4,5,6,7,8]

PEDOT:PSS, or poly(3,4-ethylenedioxythiophene):poly(styrenesulfonate) (see Figure 1), was discovered in the early 1990s during the search for stable conducting polymers.[9] PEDOT by itself is relatively conductive when oxidised on account of its planar structure which facilitates the delocalization of π electrons.[10] It also has good transparency at visible wavelengths but is insoluble in most common solvents and is easily oxidised in air which severely limits its processability.[10] Combination with PSS was found to resolve these issues by forming an ionic polymer complex with PEDOT, which facilitates the formation of a water-borne dispersion, and by acting as a counter ion to stabilise PEDOT in its oxidised (P-doped) state.[11] The PEDOT:PSS dispersion has been shown t consist of negatively charged colloidal particles 20-70nm long[12] with each particle containing several PEDOT chains. The degree of polymerization is limited with each PEDOT chain containing only 10 – 20 monomers.[13] Due to excess PSS the dispersion is acidic with a pH of approximately 2. Aqueous dispersions of PEDOT:PSS are commercially available from H. C. Stark, under the brand name Clevios and from AGFA under the name Orgacon. Clevios P, with a work function of 5.2eV is the brand of PEDOT:PSS used in this research.[14]

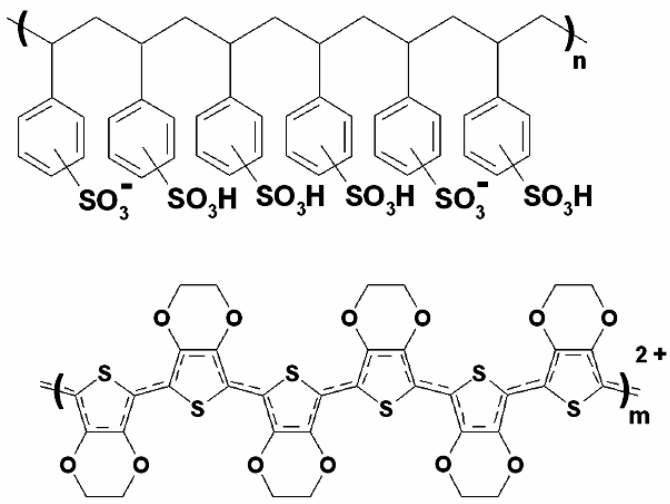

Figure 1. Molecular structures of PEDOT (below) and PSS (above)[14]

PEDOT:PSS is a highly successful thin film material, seeing use as an antistatic coating, high conductivity coatings, organic transistors, solid electrolyte capacitors and in organic light emitting diodes (OLEDs).[14] The use of PEDOT:PSS in polymer based photovoltaics stems from its use in OLEDs where it was shown to improve device lifetimes and planarise the anode, greatly reducing the number of short circuits. In addition, it provided a more suitable work function for hole injection.[10] These effects proved to be beneficial in polymer based photovoltaics as well.

Most research focusing on a highly conductive, solution processable, transparent electrode typically involves the conducting polymer PEDOT:PSS. This route has involved the addition of secondary additives to PEDOT:PSS in order to reduce its sheet resistance, while endeavouring to maintain high optical transparency. To date, this direction has yielded some success but it has previously not been investigated in conjunction with the P3HT:PCBM system.

The first reported use of modified PEDOT:PSS in organic electronics occurred in 2001 when Granlund et al.[15] used a mixture of PEDOT:PSS and sorbitol (7:13 w/w) as a high conductivity anode in a polymer light emitting diode. The researchers were studying the emission zone of a single layer, substituted polythiophene LED and chose the modified PEDOT:PSS as an alternative to ITO primarily for modelling reasons: the graded nature of ITO means that the complex index of reflection changes with depth through an ITO layer. The authors stated that this would lead to modelling complications. Instead, a PEDOT:PSS layer with enhanced conductivity was chosen as a simpler alternative.

A follow up paper was published later that year presenting AFM images and cyclic voltammograms of a glycerol modified PEDOT:PSS electrode.

In 2002 it was discovered that glycerol could greatly decrease the surface sheet resistance of PEDOT:PSS thin films[16] from 7150 Ω /□ to 1850 Ω /□ while maintaining high optical transparency. OLEDS fabricated with the modified PEDOT:PSS were far superior than control devices and at the time represented the highest external electroluminescence efficiency for a molecular OLED using a conducting polymer anode.

In 2004, Zhang et al were the first to apply modified PEDOT:PSS layers to polymer photovoltaics.[8] Both glycerol and sorbitol were investigated as additives were investigated in MEH-PPV:PCBM bilayer devices. Sorbitol proved to create better devices, but neither additive could produce results comparable to an ITO anode.

Concurrently, investigations of the underlying causes behind the improvement in conductivity that these additives provide began to bear fruit. In 2003 Jőnsson et al.[17] published a paper presenting XPS spectra of pristine PEDOT:PSS films and films from a mixture of 10g PEDOT:PSS, 0.3 g of sorbitol, 0.5 g of NMP and 10g of isopropanol. In addition, two different PEDOT:PSS brands were compared, chosen for their differing PEDOT:PSS ratios. After heat treatment, the XPS survey and core level spectra of the solvent-added films were all identical to the corresponding spectra of heat-treated pristine PEDOT:PSS films. There was also no significant difference between the spectra of 'as prepared' and heat-treated PEDOT–PSS–pristine. The authors took this evidence to suggest that the improvement in conductivity is not primarily due to chemical changes in the films.

The researchers then went on to investigate possible morphological causes for the increase in conductivity. AFM showed that films spin cast from PEDOT:PSS solutions containing additives were significantly rougher. This roughness was greatly reduced by an annealing process due to the removal of solvent molecules from the film surface. AFM results revealed increased surface roughness of the as-cast films of modified PEDOT:PSS. This roughness was attributed to solvent molecules at the film surface and was greatly reduced by annealing.

In addition, the authors note that the higher the PEDOT content, the higher the conductivity of the films, which is expected as PEDOT is the charge carrying species. The addition of the solvents drastically reduced the sheet resistance of the film by a factor of 300. Heat treating the films further enhanced the effect, leading to a three

order of magnitude reduction in sheet resistance. Furthermore, the ratio of PEDOT to PSS was increased at the surface of the films. In the solvent-added films without heat treatment the surface concentration was more than double the pristine film concentration. In the solvent-added, heat treated films, the ratio of PEDOT to PSS at the film surface was three times higher than the pristine film ratio.

In 2004 Martin et al.[18] published a paper looking at a range of hydroxylated secondary additives (SAs) in Baytron P films on PET. The SAs included thiodiethanol, diethylene glycol, glycerol, ethylene glycol, 2-methylthioethanol, 2-methoxyethanol, and salicylsulfonic acid (SSA). The SAs were first dissolved in methanol before being added to the PEDOT:PSS. The final weight ratio of SA:MeOH:Baytron P is reported as 0.05:0.14:0.81 for all SAs investigated. Interestingly, they found that adding MeOH by itself to PEDOT:PSS more than halved the sheet resistance to 1250 Ω /□. 2,2'-thiodiethanol and diethylene glycol were the most effective SAs for lowing the sheet resistance and increasing conductivity, followed by glycerol. IR specrtra of films containing 2,2'-thiodiethanol showed a tendency for styrene sulfonate moieties to preferentially adopt the ionized , $-SO_3^-$ form versus the hydrogen-bonding –SO3H form. The authors hypothesised that this may increase the number of PEDOT–PSS electrostatic pairing events, causing an increase in film stability and subtle changes in the molecular ordering of the PEDOT units, which in turn lead to a decreased film resistance. Results of immersion test in methanol-*d* were also consistent with the idea that the 2,2'-thiodiethanol doped films adopting increased electrostatic pairing at the expense h-bonding interactions. XRD results showed no increased crystallinity in the doped films.

Lastly, In 2005 Snaith et al.[19] published research detailing the use of a G-PEDOT anode in a polymer-polymer photovoltaic device (F8BT and PFB). Glycerol was added to PEDOT:PSS at a concentration of 8% by volume. The authors used PEDOT:PSS from an undisclosed source with a low weight ratio of 1:16 PEDOT to PSS. AFM revealed that small (40nm) particles of PEDOT:PSS became swollen and aggregated when glycerol was added. FTIR spectra showed that all the glycerol was removed from the film by heat treating, suggesting that all electronic changes were due to structural changes in the PEDOT:PSS. EQE results showed a significant improvement in devices with a G-PEDOT electrode. An increase in V_{OC} from 1.1V to 1.3V was also reported. Kelvin probe microscopy was used to show that the surface potential of the G-PEDOT film was, on average, 120mV less than the PEDOT film. This shift was used to support the claim that the PSS is more evenly distributed vertically within the G-PEDOT film than in the PEDOT film where there is a tendency for the PEDOT and PSS to stratify, forming a PSS rich surface.

V.II Hypothesis

Considering the significant reduction in sheet resistance, improvements in optical transmission and photovoltaic parameters that have been reported due to the addition of glycerol to PEDOT:PSS, it was hypothesised that glycerol modified PEDOT:PSS anodes may prove beneficial in P3HT:PCBM solar cells, by improving light transmission and reducing the series resistance through the anode layer. To test this P3HT:PCBM solar cells incorporating glycerol modified PEDOT:PSS anodes were fabricated and tested.

V.III Methods

To test the effect of glycerol modified PEDOT:PSS anodes on P3HT:PCBM solar cell efficiency, photovoltaic devices were fabricated according to the method outlined in Chapter 3 incorporating G-PEDOOT anodes spin cast from solutions of varying glycerol concentration. Glycerol (Fisher, >99.5%) was added to 300 μL of methanol (Sigma, >99.9%) and stirred, before being added to 2mL of PEDOT:PSS (HC Starck, Clevios P). Glycerol concentrations of 0.08, 0.5, and 1.45 mg/mL PEDOT:PSS were investigated. Experiments at higher concentrations were abandoned due to excessive viscosity. In order to maintain a constant film thickness, the spin casting speed was varied. Spin speeds of 5000, 4000 rpm, 2500 and 1000 rpm were used for PEDOT:PSS solutions containing glycerol concentrations of 0, 0.08. 0.5 and 1.45 mg/mL, respectively.

PEDOT:PSS was wiped off those areas of the substrate where the cathode contact pins to rule out the possibility that the contact pins may penetrate the aluminium and polymer:fullerene layer and partially short the devices.

UV-VVIS transmission spectra of G-PEDOT modified films on ITO glass were measured on a Cary 5000 UV-visible-NIR spectrometer. ITO coated glass substrates were used as blanks.

I-V curves were measured using a 150W Newport Solar Simulator as outlined in Chapter 3. Subsequently, masked I-V curves were also measured, whereby a mask

with a 1mm diameter hole was used to ensure that light was only incident on the defined pixel area. The dark side of the masking plate was painted black in order to minimise the effect of any internal reflections.

Dark I-V curves were modelled by fitting to the standard one diode solar cell model:[20]

$$I = I_0\left[e^{q(V-IR_S)/nk_BT} - 1\right] + \frac{V - IR_S}{R_{SH}} \quad (1)$$

Where I is the current through the solar cell, I_0 the reverse saturation current, k_B is Boltzmann's constant, T the temperature in Kelvin, V the external bias applied to the device, n the diode ideality factor, R_S the series resistance and R_{SH} is the shunt resistance. R_S and R_{SH} were estimated as explained in Chapter 3. The built in voltage of a solar cell, V_{bi}, defined as the voltage at which the photocurrent equals zero was determined, where the photocurrent was calculated by subtracting the device current measured in the dark, subtracted from the device current measured under illumination.

Spatially resolved I-V curves were also conducted. By using an iris and two plano-convex lenses, the I-V characteristics for various spot sizes of incident radiation were recorded. The experimental set up is presented in Figure 2 and was calibrated to ensure that the flux at the device plane was 40mW/cm^2.

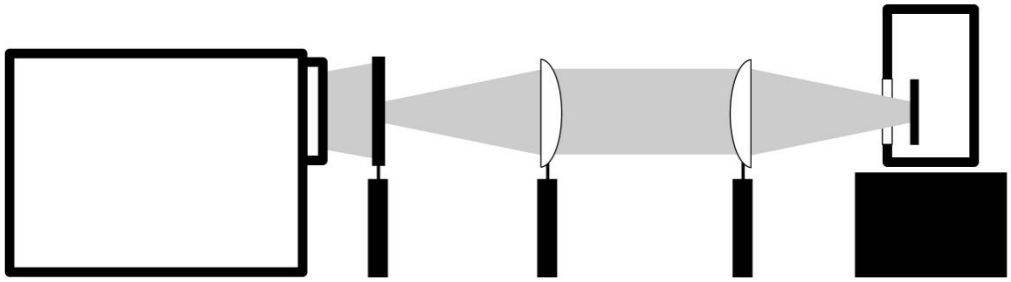

Figure 2. Experimental Setup for the spatially resolved I-V curves

External quantum efficiency spectra were measured as outlined in Chapter 3 and estimated AM1.5G J_{SC} values were calculated by integrating the EQE curve across the AM1.5G spectra. Sheet resistance values were determined for modified and unmodified PEDOT:PSS films using a custom made four point probe set-up as outlined in Chapter 3. Surface morphology was investigated by AFM and optical interferometry using a Parks Scientific Instruments CP-II AFM in non-contact mode and a MicroXAM 5000 3D surface profiler respectively.

V.IV Results and Discussion

V.IV.I UV-Visible Transmission Spectra of Glycerol Modified PEDOT:PSS films

As discussed earlier, some reports have noted an improvement in optical transmission in glycerol modified PEDOT:PSS films. As such, UV-VIS transmission spectra were measured herein, in order to determine any effect that the glycerol modification may have on the optical properties of the PEDOT:PSS layer (Figure 3). As can be seen, all the devices have virtually identical transmission spectra, with no sign of improved transmission in the glycerol modified films. It is possible that the

previously reported improvement in optical transmission was simply the result of a reduction in film thickness resulting from the addition of glycerol. Film thickness measurements taken with a Dektak profilometer showed that all PEDOT:PSS and G-PEDOT:PSS films used in this study were 40 ±3nm thick. Although pure glycerol has a boiling point of 290°C, FTIR spectra of glycerol-modified films has shown that a heat treatment at 120°C is capable of removing all the glycerol from the PEDOT:PSS film.[19] From the UV-Vis transmission spectra presented here, one can infer that the glycerol modification has no impact on the optical transmission of PEDOT:PSS over the wavelength range relevant to the photoactive layer. As a result, optical effects can be ruled as a potential cause of any subsequent changes in device efficiency.

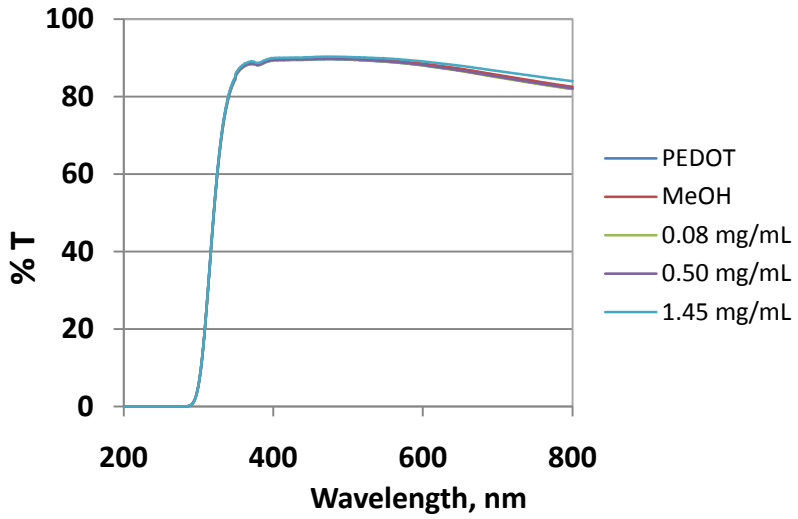

Figure 3. UV-Vis Transmittance spectra of PEDOT and G-PEDOT films on ITO coated glass. Also included is the spectrum of a film spun from a PEDOT:PSS solution containing methanol but no glycerol.

V.IV.II Un-masked I-V curves and EQE of Modified Devices

Un-masked J-V curves conducted on the P3HT:PCBM solar cells containing glycerol modified PEDOT:PSS presented very interesting results. As shown in Figure 4, a large increase in the J_{SC} from 9.3 mA/cm^2 to nearly 24.9 mA/cm^2 was observed, in conjunction with a small drop in V_{OC}. Although the drop in V_{OC} is small, it was consistently seen across all tested devices. It is possible that the depressed V_{OC} could be due to a glycerol induced reduction in the PEDOT:PSS work function. Previously reported Kelvin probe microscopy measurements have indicated a work function reduction of 0.1 eV from 5.5eV to 5.4eV,[19] which is far greater than the 0.02V reduction in V_{OC} observed here. A reduction in the PEDOT:PSS work function might be expected to effect the built in voltage, V_{bi}, of the photovoltaic device. However, calculations of the V_{bi} for both PEDOT and G-PEDOT based devices found no significant difference between the two, indicating that, in this case, either the PEDOT:PSS work function is not affected by glycerol addition, or that small variations in the PEDOT:PSS work function have no significant effect on the V_{OC}.

Analysis of the dark I-V curves reveals a better explanation for the reduced V_{OC}, with the G-PEDOT device exhibiting a much higher dark current (Figure 5). By modelling the dark I-V curves with the standard one diode solar cell model (Equation 1) a value for the reverse saturation current, I_0, can be extracted, with a significantly larger value of 3 x 10^{-10} A obtained for the G-PEDOT device compared to 5 x 10^{-11} A for the PEDOT device. Rearrangement of the standard one diode solar cell model reveals that the V_{OC} is dependent on the ratio of I_{SC}/I_0, according to:

$$V_{OC} = \frac{nkT}{q} \ln\left[\frac{1}{I_0}\left(I_{SC} - \frac{V_{OC}}{R_P}\right) + 1\right] \quad (2)$$

Given that the ratio of I_{SC}/I_0 is smaller for the G-PEDOT device, one could expect to observe a smaller V_{OC}. Plugging the numbers into the model (n = 1.552), one obtains calculated V_{OC}s of 0.581 and 0.609 for the G-PEDOT and PEDOT based devices respectively, which match well with the measured values.

In addition to a slightly depressed V_{OC}, the G-PEDOT based device shows significantly reduced series and shunt resistances, the origins of which will be discussed later.

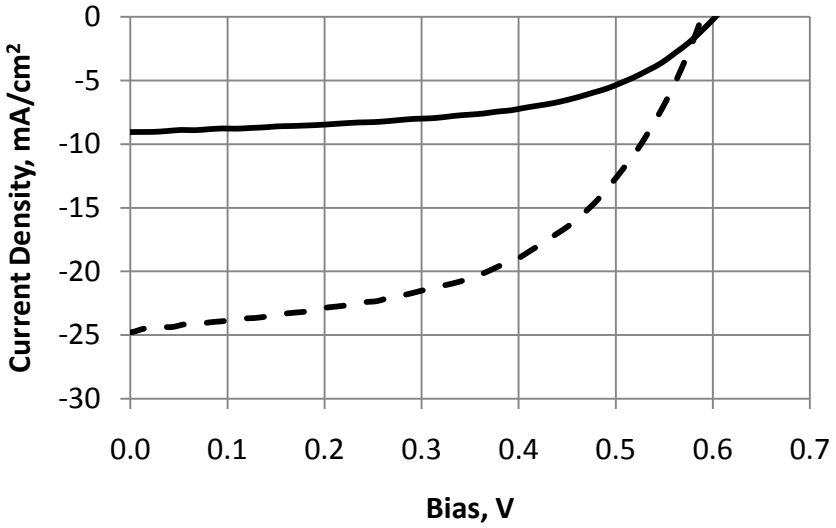

	J_{SC}, mA/cm²	FF	V_{OC}, V	PCE, %	R_S, Ω	R_{SH}, KΩ	V_{bi}
PEDOT	9.1	0.54	0.60	3.0	380	11.1	0.70 ± 0.03
G-PEDOT	24.9	0.52	0.58		160	5.2	0.70 ± 0.02

Figure 4. J-V curves and parameters of a glycerol modified (0.03 mg glycerol/mL PEDOT:PSS) ((dotted line) and un-modified (bold line) P3HT:PCBM solar cells, and device parameters. R_{SERIES} and R_{SHUNT} values are estimates derived from I-V curves, as outlined in Chapter 3.

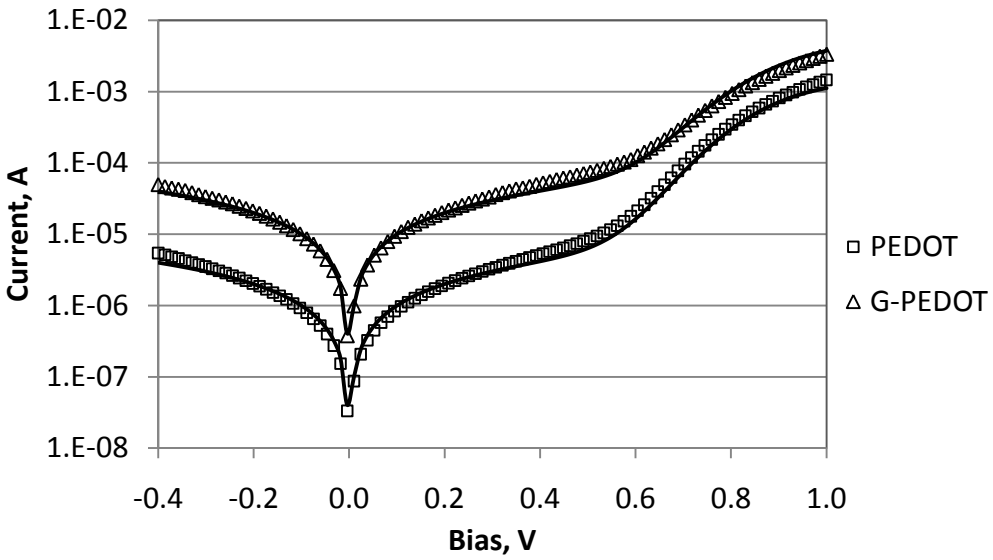

Figure 5. Dark I-V curves fitted with the standard one diode solar cell model.

V.VI.III EQE Spectra

EQE spectra were measured to determine the validity and origin of the G-PEDOT based device's extremely high J_{SC}. As Figure 6 shows, the EQE spectra of all the devices are very similar, in contrast to the experimentally determined I-V curves. By integrating the EQE curves across the AM1.5G spectrum, estimated J_{SC} values of only 7.3 – 7.7 mA/cm^2 were calculated, throwing doubt on the measured J_{SC} values. In addition, it can be shown that the measured J_{SC} of 24.9 mA/cm^2 exceeds the theoretical maximum of 16.8 mA/cm^2 for a P3HT based solar cell.[21]

It was initially hypothesised that the increased G-PEDOT conductivity may allow cross talk between pixels on the device, thereby boosting the J_{SC}. However, substrates prepared with only one pixel still showed unfeasibly high J_{SC}s.

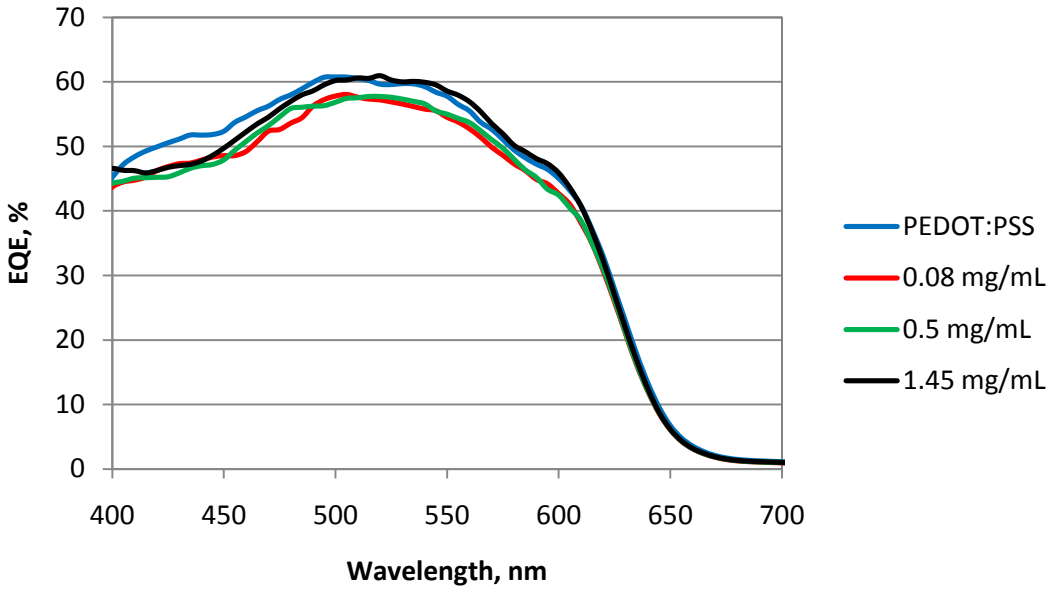

Figure 6. External Quantum Efficiency of P3HT:PCBM devices with various PEDOT:PSS layers

However, in actual fact, the disparate J-V and EQE data result from differences in the I-V and EQE experimental setups. In the I-V experiment, the source illuminates nearly the entire substrate area, including all three solar pixels. For the purposes of calculation, the device area is defined as the area of overlap between the ITO and Aluminium strips. In contrast, in the EQE setup, the source is monochromated, shaped by an iris and then focused onto an individual pixel such that no light is incident on any other part of the substrate. Figure 7shows the area over which light falls in each of the experiments.

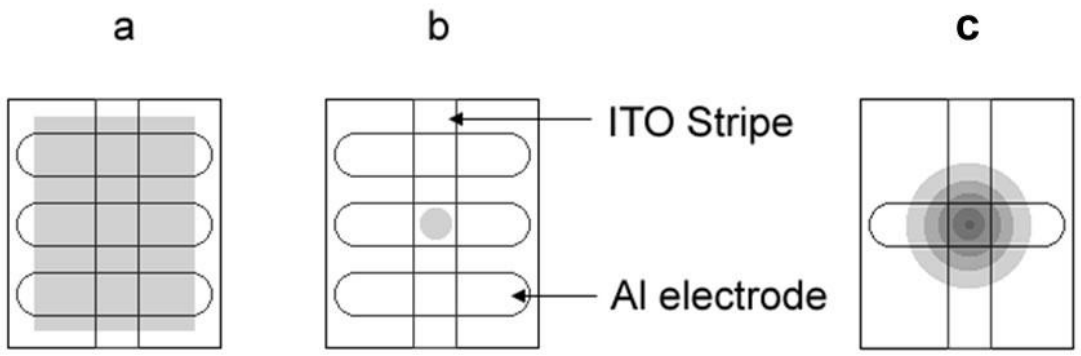

Figure 7. Schematic showing incident light patterns (shaded area) on substrates in the IV setup (a), EQE setup (b) and for spatially resolved photocurrent measurements (c).

The results suggest that the glycerol modified PEDOT:PSS layer allows the device to extract charge carriers that are generated outside the pixel boundary, leading to an inflated J_{SC} value. Sheet resistance values of pristine and glycerol modified PEDOT:PSS films are presented in Table 1 and show that glycerol modification reduces the sheet resistance by almost three orders of magnitude to 3 - 4 kΩ/□. Although still significantly higher than the 10 – 20 Ω/□ typical of ITO, the glycerol modified PEDOT:PSS is conductive enough to act as a 'pseudo ITO', implying that any part of the photoactive layer that is coated with Al could be contributing to the current. This also explains the inflated dark current, and reverse saturation currents in the G-PEDOT devices, as the pixel area is effectively much larger in these devices.

Building on work by Cravino et al,[22] It is possible to investigate the distance over which extra current can be recruited. The aluminium cathode of the devices is 0.15cm wide, the PEDOT:PSS layer is 40 nm thick and the four point probe measurements of the G-PEDOT films revealed a resistivity value, ρ, of 0.006 Ωcm.

The resistance through the G-PEDOT film (parallel to the plane of the device) can be calculated according to:

$$R = \frac{\rho L}{A} \tag{3}$$

Where ρ is the resistivity, L is the length through the conductor and A is the conductor cross sectional area. From Equation 2, the resistance through the G-PEDOT layer can be calculated as a function of distance from the ITO, according to:

$$\mathrm{R} = 0.11 \times \frac{0.00006}{0.0015 \times 40 \times 10^{-9}} \mathrm{L} \tag{4}$$

$$\mathrm{R} = 125{,}000\mathrm{L} \tag{5}$$

Where the factor of 0.11 is included to recognise that the effective resistance is lowered due to the fact that the width of the G-PEDOT film (14 mm) is actually nine times larger than the width of the Al electrode (1.5 mm). The voltage drop required to move a certain current can then be determined as a function of distance from the ITO anode according to:

$$\mathrm{V} = \mathrm{I} \times 125{,}000\mathrm{L} \tag{6}$$

Taking a typical I_{SC} of 740 μA for a glycerol modified device, compared to 240 μA for an un-modified device, 500 μA must be recruited from the active layer surrounding the assumed pixel area, or 250 μA from each side of the ITO stripe. According to Equation 4, a current of 250μA induces a voltage drop of only 0.125V over 4mm,

which is comparable to the difference between the work functions of PEDOT:PSS and ITO and indicates that the G-PEDOT anode allows significant current to be extracted several millimetres from the ITO strip.

V.VI.IV Spatially Resolved Current Measurements

The spatially resolved current measurements presented in Figure 8 directly support this analysis. At low spot diameters, smaller than the pixel diameter, the photocurrent increases linearly for both pristine and modified PEDOT based devices, as the spot spreads out over the defined pixel area. In the un-modified device, as the spot size expands beyond the pixel boundary, the I_{SC} levels out at 0.1mA. By contrast, in the glycerol modified device, the current continues to increase linearly with the spot diameter, all the way to the edge of the substrate. It is clear that the greatly reduced sheet resistance of the G-PEDOT:PSS layer allows the recruitment of current from far beyond the edges of the pixel area, and is the cause of the deceptively large J_{SC} values presented earlier.

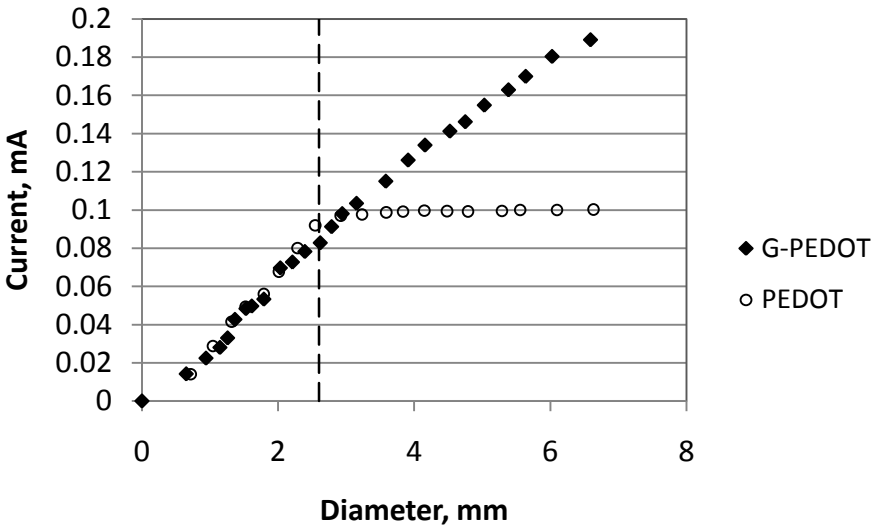

Figure 8. Spatially resolved current measurement of modified (diamond) and un-modified (square) P3HT:PCBM solar cells as a function of the light spot area. The light spot crosses the pixel edge at a beam diameter of 2.6mm

V.VI.V Masked I-V Curves of Glycerol modified Devices

In order to obtain more accurate I_{SC} values for the glycerol modified devices, the white light setup was modified by the addition of a masking plate which was placed directly onto top of the glass substrate. As a result the device area was defined by the area of the hole in the blocking plate with no light incident outside of this area. The dark side of the masking plate was painted black in order to minimise the effect of any internal reflections. Subsequently, a number of devices containing glycerol modified PEDOT:PSS were tested and the I-V parameters are recorded in Table 1. The results show that the addition of glycerol to the PEDOT:PSS layer had no significant effect on device efficiency for any of the concentrations tested. However, two significant trends can be identified. Firstly, that the addition of glycerol is correlated with a slight reduction in V_{OC}, and secondly, that the addition of glycerol is

correlated with a significant reduction in the shunt resistance, yet the series resistance is not significantly affected.

As previously determined, the depressed V_{OC} is most likely due to the large dark current in the G-PEDOT based devices which is facilitated by the much larger effective device area. From the calculated sheet resistance values it is possible to determine the contribution of the PEDOT:PSS film to the series resistance through the device (perpendicular to the plane of the device), according to Equation 2. As determining an exact value for A, the device area, is difficult for the G-PEDOT devices, the area of the device pixel is used (1.5mm x 2 mm). As a result, the calculated resistance values are conservatively high. For the four device types investigated, series resistances through the PEDOT:PSS layer of 0.5 $m\Omega$, 0.8 $\mu\Omega$, 0.7 $\mu\Omega$ and 0.9$\mu\Omega$ respectively were calculated, which are all insignificant in comparison to the overall series resistance which is on the order of 200Ω. As a result it is unlikely that glycerol modified PEDOT:PSS should have any discernible effect on the series resistance through the device and this is borne out by the experimentally estimated series resistance values presented in Table 1.

Glycerol conc. (mg/mL)	0	0.08	0.5	1.45
J_{SC} (mA/cm2)	8.4±0.3	8.0±0.3	8.4±0.2	8.4±0.2
J_{SC} est. From EQE	7.7	7.3	7.5	7.6
V_{OC} (V)	0.63	0.58	0.60	0.59
FF	0.55±0.1	0.53±0.02	0.52±0.1	0.52±0.03
PCE (%)	2.9±0.2	2.5±0.2	2.6±0.1	2.6±0.3
R_{SERIES}, Ω	194 ± 16	197 ± 19	203 ± 23	202 ± 16
R_{SHUNT}, kΩ	15.1 ± 1.2	9.1 ± 0.9	9.2 ± 1	9.7 ± 0.7
RMS Roughness (nm)	1.1±0.5	2.0±0.4	4.9±0.6	8.5±0.6
Sheet Resistance (kΩ/sq.)	2320	3.7	3	4.35

Table 1. J-V and other characteristics for devices containing PEDOT:PSS layers modified with various concentrations of glycerol. R_{SERIES} and R_{SHUNT} values are estimates derived from I-V curves.

V.VI.VI Surface Topography

In an effort to shed light on the cause of the reduced shunt resistance, the surface topography of the PEDOT and G-PEDOT films was investigated by AFM and optical interferometry. One of the functions of the PEDOT:PSS film in a polymer based photovoltaic device is to act as an electron blocking layer which reduces the leakage current at forward bias and therefore improves the shunt resistance. Alterations to the film topography could conceivably affect the films ability to fulfil this role and lead to the observed reduction in shunt resistance.

V.VI.VI.I Atomic Force Microscopy

The atomic force micrographs show a clear correlation between the glycerol concentration and surface roughness on the micrometer scale, similar to results observed by other researchers.[19] The correlation is quantified by RMS roughness

measurements that were extracted from the atomic force micrographs and are represented in Table 1. The RMS roughness is shown to increase from 1.1 ± 0.5 nm for PEDOT films to 8.5 ± 0.6 nm for the most concentration G-PEDOT film. As the PEDOT:PSS film is only 40m thick, It is possible that the increased surface roughness observed in G-PEDOT films could lead to localised areas of thinning that are less effective at blocking electrons, leading to an increased leakage current and shunt resistance. However, if this was so, one would expect to see a gradual decline in the shunt resistance, which correlates with the gradual increase in RMS roughness. However, this is not the case, with the shunt resistance exhibiting a sharp drop on the introduction of glycerol, which then remains consistently low, independent of further increases in glycerol concentration.

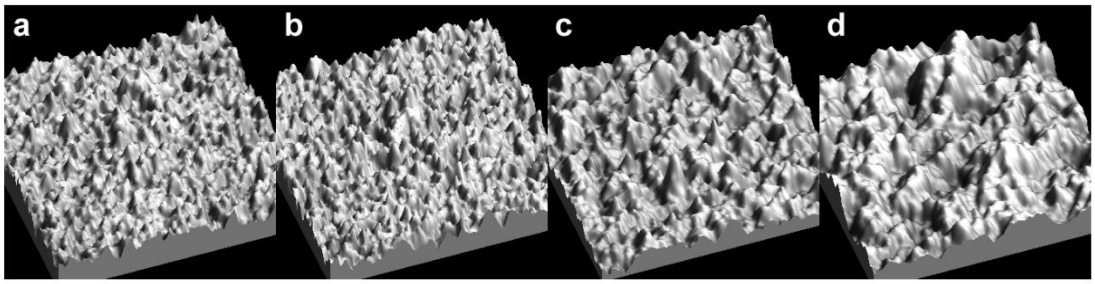

Figure 9. Characteristic atomic force micrographs of PEDOT:PSS films on ITO glass with varying levels of glycerol doping; 0 mg/mL (a), 0.08 mg/mL (b), 1.0 mg/mL (c), 1.45 mg/mL (d).

V.VI.VI.II MicroXAM analysis of Glycerol modified PEDOT:PSS Films

Optical interferometry allowed the film topography to be investigated on a larger scale and revealed a more likely explanation in the form of glycerol induced micro craters, as shown in Figure 9. The un-modified film in Figure 10A displays a very flat

surface with no interesting surface features. However, in Figure 9B, the introduction of glycerol is correlated with the appearance of micro craters. Figure 9E presents a line profile of a typical micro crater which is 40 ± 11μm wide and 17 ± 4nm deep. The craters are most likely formed by excess glycerol that does not fully dissolve into the methanol/PEDOT:PSS due to its high viscosity. These glycerol bubbles remain in the film after it has been spin cast and then boil off during the PEDOT heat treatment, leaving behind the micro craters. The craters create localised regions where the PEDOT:PSS layer is 50% thinner than the pristine PEDOT:PSS. This is likely to reduce the electron blocking efficacy of the PEDOT:PSS film and cause the reduced shunt resistance.

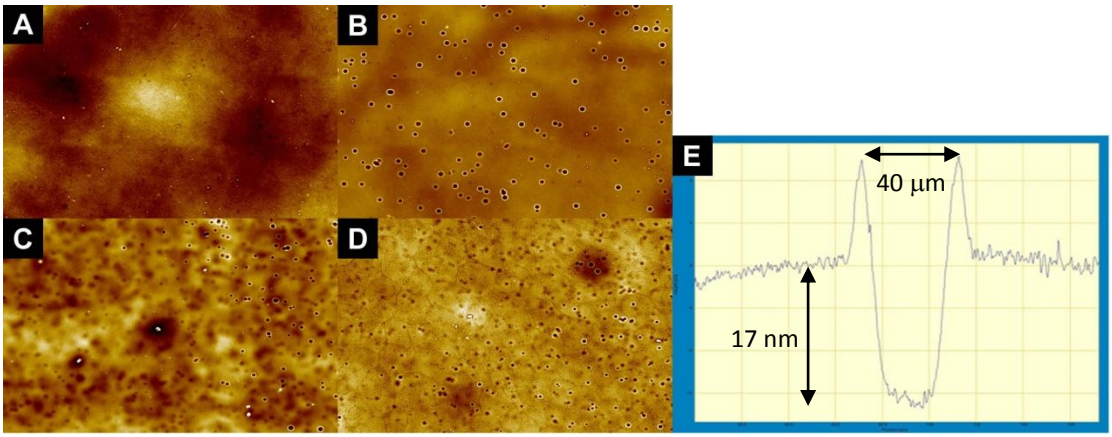

Figure 10. Micro XAM optical interferometry images of PEDOT:PSS and G-PEDOT:PSS films.; A = 0 mg/mL, B = 0.08 mg/mL, C = 1.0 m/mL, D = 1.45 mg/mL. Images are 2.5 x 2.5 mm. On the right is a line profile of a crater from image C. The craters is 40 ± 11μm wide and 17 ± 4nm deep

V.VIII Conclusions

In conclusion, glycerol modified PEDOT:PPS films have been investigated for use as transparent anodes in P3HT:PCBM solar cells. Initial results proved to be theoretically impossible and highlighted a potential weakness in the I-V experimental set-up. Once corrected, subsequent tests showed that the use of glycerol modified PEDOT:PSS anodes provided no significant benefit to the overall of P3HT:PCBM solar cells. Sheet resistance measurements showed a drastic reduction in PEDOT:PSS sheet resistance due to glycerol modification, which in turn led to current scavenging from outside the assumed pixel area. Spatially resolved photocurrent measurements showed that current was scavenged from as far as 4 mm from the pixel edge. AFM images showed increased roughness with increased doping concentration while optical interferometry revealed the formation of novel micro craters which are ascribed to the evaporation of undissolved glycerol bubbles in the PEDOT:PSS film. These micro craters are most likely responsible for the reduced shunt resistance in G-PEDOT based devices.

V.IX References

[1] Park, S., Tark, S. J., Lee, J. S., Lim, H. & Kim, D. Effects of intrinsic ZnO buffer layer based on P3HT/PCBM organic solar cells with Al-doped ZnO electrode. *Solar Energy Materials and Solar Cells* **93**, 1020-1023 (2009).

[2] Lee, C. *et al.* IZO/Al/GZO multilayer films to replace ITO films. *Journal of Materials Science: Materials in Electronics* **19**, 981-985 (2008).

[3] Sahu, D. R. & Huang, J.-L. Development of ZnO-based transparent conductive coatings. *Solar Energy Materials and Solar Cells* **93**, 1923-1927 (2009).

[4] Pasquier, A. D., Unalan, H. E., Kanwal, A., Miller, S. & Chhowalla, M. Conducting and transparent single-wall carbon nanotube electrodes for polymer-fullerene solar cells. *Applied Physics Letters* **87**, 203511 (2005).

[5] Rowell, M. W. *et al.* Organic solar cells with carbon nanotube network electrodes. *Applied Physics Letters* **88**, 233506 (2006).

[6] Wu, J. *et al.* Organic solar cells with solution-processed graphene transparent electrodes. *Applied Physics Letters* **92**, 263302 (2008).

[7] Wang, X., Zhi, L. & Mullen, K. Transparent, Conductive Graphene Electrodes for Dye-Sensitized Solar Cells. *Nano Letters* **8**, 323-327, doi:10.1021/nl072838r (2007).

[8] Zhang, F. L., Johansson, M., Andersson, M. R., Hummelen, J. C. & Inganas, O. Polymer photovoltaic cells with conducting polymer anodes. *Advanced Materials* **14**, 662-665 (2002).

[9] Gerhard Heywang & Friedrich Jonas. Poly(alkylenedioxythiophene)s - new, very stable conducting polymers. *Advanced Materials* **4**, 116-118 (1992).

[10] Kok, M. M. d. *et al.* Modification of PEDOT:PSS as hole injection layer in polymer LEDs. *physica status solidi (a)* **201**, 1342-1359 (2004).

[11] Ghosh, S. & Inganas, O. Nano-structured conducting polymer network based on PEDOT-PSS. *Synthetic Metals* **121**, 1321-1322 (2001).

[12] Elschnet, A., Jonas, F., Kirchmeyer, S. & Wussow, K. in *Asia Display IDW 2001.* 1427-1429.

[13] Dietrich, M., Heinze, J., Heywang, G. & Jonas, F. Electrochemical and spectroscopic characterization of polyalkylenedioxythiophenes. *Journal of Electroanalytical Chemistry* **369**, 87-92 (1994).

[14] *Clevios P*, <http://www.clevios.com/index.php?page_id=995&prod_service_id=317&anw_id=&operate=&suchfeld=&suchstart=602&prodselect_5=317|> (

[15] Granlund, T., Pettersson, L. A. A. & Inganas, O. Determination of the emission zone in a single-layer polymer light-emitting diode through optical measurements. *Journal of Applied Physics* **89**, 5897-5902 (2001).

[16] Kim, W. H. *et al.* Molecular organic light-emitting diodes using highly conducting polymers as anodes. *Applied Physics Letters* **80**, 3844-3846 (2002).

[17] Jonsson, S. K. M. *et al.* The effects of solvents on the morphology and sheet resistance in poly (3,4-ethylenedioxythiophene)-polystyrenesulfonic acid (PEDOT-PSS) films. *Synthetic Metals* **139**, 1-10 (2003).

[18] Martin, B. D. *et al.* Hydroxylated secondary dopants for surface resistance enhancement in transparent poly(3,4-ethylenedioxythiophene)poly(styrenesulfonate) thin films. *Synthetic Metals* **142**, 187-193 (2004).

[19] Snaith, H. J., Kenrick, H., Chiesa, M. & Friend, R. H. Morphological and electronic consequences of modifications to the polymer anode 'PEDOT : PSS'. *Polymer* **46**, 2573-2578 (2005).

[20] Schilinsky, P., Waldauf, C., Hauch, J. & Brabec, C. J. Simulation of light intensity dependent current characteristics of polymer solar cells. *Journal of Applied Physics* **95**, 2816 (2004).

[21] Smestad, G. P. *et al.* Reporting solar cell efficiencies in Solar Energy Materials and Solar Cells. *Solar Energy Materials and Solar Cells* **92**, 371-373 (2008).

[22] Cravino, A., Schilinsky, P. & Brabec, C. J. Characterization of Organic Solar Cells: the Importance of Device Layout. *Advanced Functional Materials* **17**, 3906-3910 (2007).

V.X Appendix

V.XI.I Four point probe measurements of PEDOT:PSS and G-PEDOT:PSS Sheet Resistance, from which the sheet resistance values in Table 1 were calculated

V.XI.I.I. PEDOT:PSS

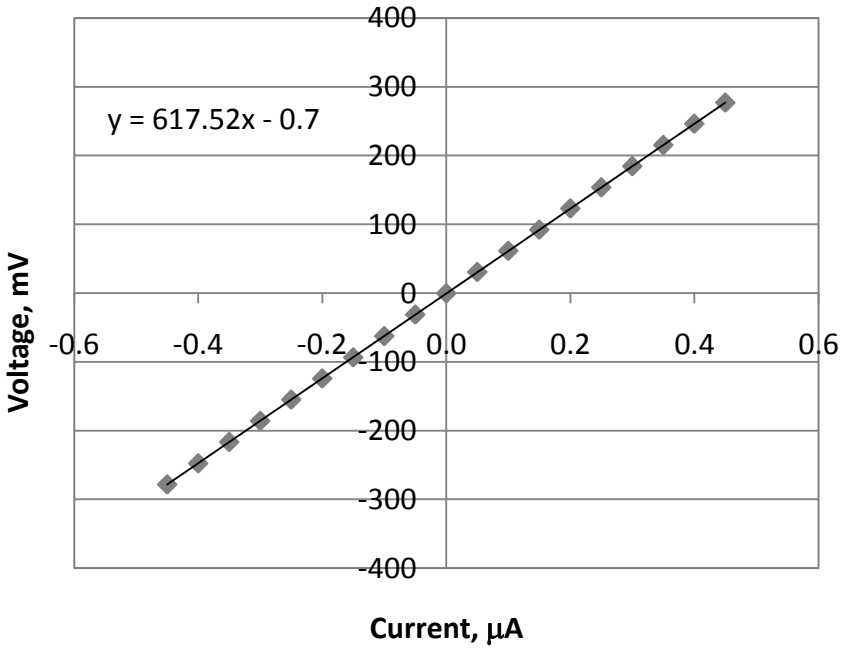

V.XI.I.II G-PEDOT:PSS, 0.08mg/mL

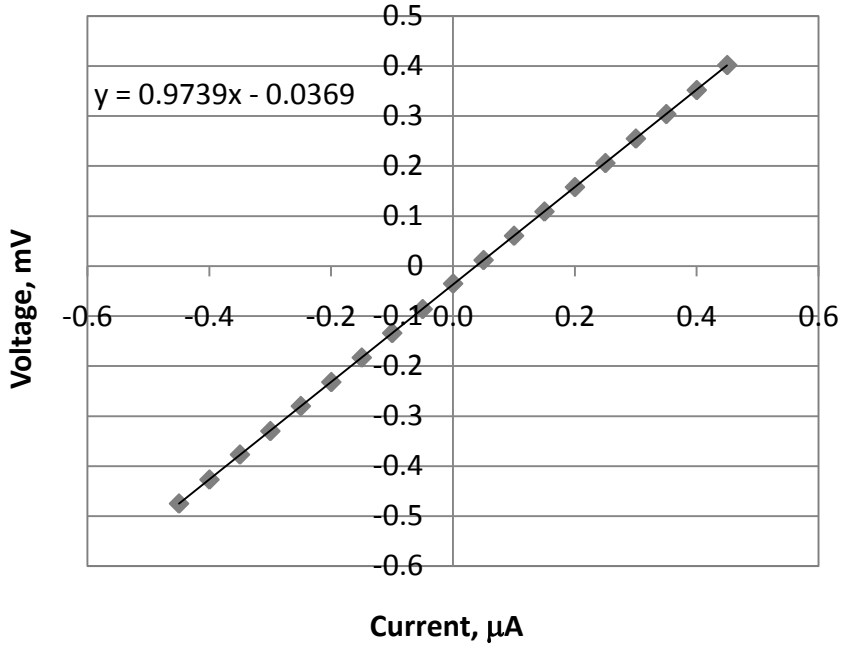

V.XI.I.III G-PEDOT:PSS, 0.5 mg/mL

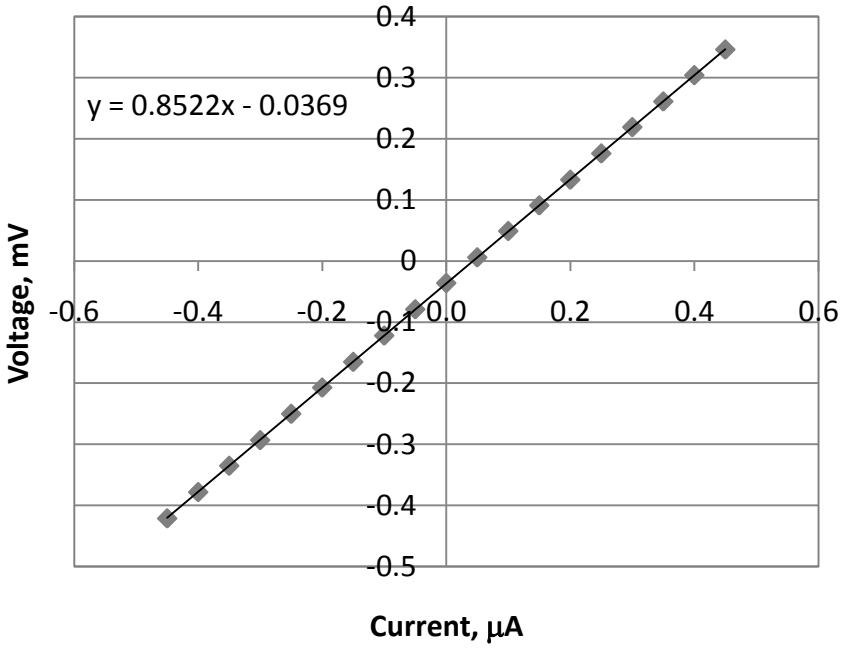

V.XI.I.III G-PEDOT:PSS, 1.45 mg/mL